Materials Chemistry and Physics 371 (2027) 133178

Contents lists available at ScienceDirect

Materials Chemistry and Physics

journal homepage: www.elsevier.com/locate/matchemphys

Electrical conductivity-based kinetic modeling for monitoring carbamide dissolution from porous metallic materials

Nuray Beköz Üllen *, Gizem Karabulut Şevk, Ali Can Özarslan

Istanbul University-Cerrahpaşa, Faculty of Engineering, Department of Metallurgical and Materials Engineering, Istanbul, Turkey

HIGHLIGHTS

- Carbamide dissolution in green porous metals was monitored by electrical conductivity.
- Dissolution kinetics varied with porosity, showing order-dependent transitions.
- Low-porosity samples followed 2nd-order interaction-controlled kinetics.
- High-porosity samples showed 1st-order diffusion-controlled behavior.
- Conductivity-based modeling offers a simple, environmentally friendly monitoring approach.

GRAPHICAL ABSTRACT

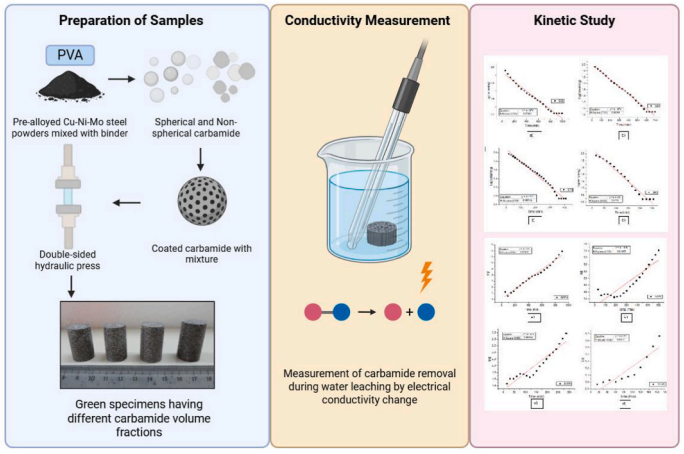

ARTICLE INFO

Keywords:
Porous metal
Conductivity
Kinetic modeling
Carbamide
Dissolution

ABSTRACT

The production of porous metal structures using space holder-water leaching technique in powder metallurgy offers many advantages, such as controlling pore morphology such as size and shape, and adjusting the ratio of open to closed pores. This technique is considered as lower-risk, environmentally friendly and control pores structures and porosity level. Using carbamide as space holder possesses numerous advantages such as low cost, fast dissolution in water and free toxicity. In this study is about the carbamide removal process as one of the most important production steps for pore structures. The green specimens with 50-80 vol% porosity were immersed in distilled water at room temperature to leach the carbamide. This process not only reduced processing time but also eliminated harmful gases released, resulting in a greener production process. The amount of carbamide dissolved in porous structures with varying porosities was determined by conductometry. More than 90% of the carbamide could be removed for theoretical porosities of 70 vol% and 80 vol%. About 15% to 25% carbamide remained in the green specimens for theoretical porosities of 50 vol% and 60 vol%. This study is important for understanding the effect of carbamide ratio and shape on the dissolution process in removing spacers from green structures. The dissolution behavior followed second-order kinetics at lower porosity levels, indicating interaction-controlled release, while higher porosity specimens exhibited first-order kinetics governed

* Corresponding author.
E-mail address: nbekoz@iuc.edu.tr (N. Beköz Üllen).

https://doi.org/10.1016/j.matchemphys.2026.133178
Received 1 December 2025; Received in revised form 2 September 2026; Accepted 27 September 2026
Available online 29 September 2026
0254-0584/© 2026 Elsevier B.V. All rights are reserved, including those for text and data mining, AI training, and similar technologies.

predominantly by diffusion. This transition reflects the crucial role of pore connectivity and morphology in determining the dissolution rate of carbamide within green metallic structures. Understanding the dissolution kinetics of carbamide is crucial for developing reliable models to understand its dissolution mechanism.

1. Introduction

Porous metals and metal foams are preferred for many structural and functional applications due to their light weight, high specific surface area, and good energy absorption properties [1,2]. For structural applications, the most important property of metal foams is the pore properties. Porous metallic structures are preferred in many areas such as automotive, space and aviation due to their unique specific mechanical properties [3–6]. Many technologies are available to produce porous metals [3]. Metals can be transformed into porous structures through either liquid- or solid-state metallurgy routes, owing to their ease of processing [7,8]. The liquid route methods are more suited to metals of relatively low melting points, such as aluminum. However, most porous metals of higher melting points, such as steel, nickel, and titanium need to be produced by solid route technologies such as powder metallurgy. The factors that cause this situation are the technical difficulties encountered in processing liquid metals at high temperatures, high processing costs and some undesirable properties realized through liquid routes. Powder metallurgy solid route methods have been used in the production of porous steel and titanium, where space holder particles are removed by dissolution or thermal processing [6,9,10]. There are two types of space holder material, such as low temperature evaporative and water leachable materials. Among the methods, the space holder-water leaching technique in powder metallurgy is a simple and cost-effective method, which can easily control shape and size. In this method, the metal powders are firstly coated or mixed with the space holder, and the compaction process is carried out subsequently. Among the water leachable space holders, urea (carbamide) is a very attractive space holder material due to its low melting point (150 °C) and high solubility in water, primarily due to its polar nature and the ability to form hydrogen bonds with water molecules [11]. Additionally, carbamide is a very low-cost material [7,10,12–15]. Many researchers have produced different metallic foams using carbamide as space holders. Several researchers have successfully fabricated steel foams with porosity levels between 50% and 80% using the space holder–water leaching technique, in which carbamide particles served as the space holder material. It is observed from these studies that morphology, as well as pore size and shape, depend on the space holder particle morphology. The porosity content can be tailored by varying the amount of space holder particles. Therefore, the selection of the space holder and its removal from the porous structure are very important.

The removal of carbamide has mostly been carried out by thermal treatment for sintering methods. In this method, carbamide is vaporized or decomposed at high temperatures, but the toxic gases that emerge during this process pose risks to the environment and health [16]. In addition, the integrity of the porous structure can be damaged by the effect of heat [14]. At elevated temperatures, for instance, primary reaction products are known to exhibit high reactivity and undergo a series of secondary reactions. Therefore, lower-risk and environmentally friendly alternatives are being investigated. Another method is dissolution with a suitable solvent. However, it is important to examine the solubility of carbamide. In literature, general methods used for the determination of carbamide in any solution are divided into four categories: urease-Kjeldahl or Nesslerization method, hypobromite manometric method, p-dimethylamino benzaldehyde or diacetyl spectrophotometry and chromatographic method [17]. The accuracy and applicability of these methods are often limited by the presence of colored or mixed substances, procedural complexity, and the narrow testing range of carbamide concentration. In response to these limitations, the conductivity method was developed as a more effective alternative. Due to the potential for oxidation, especially in metallic materials upon exposure to the solution, the gravimetric method may yield inaccurate results. Furthermore, water that penetrates the pores due to interconnections cannot dry completely, resulting in weight gain. Consequently, the use of conductivity variation as a means of determining carbamide concentration offers a more reliable and precise alternative. Numerous scientific studies have been conducted on both the dissolution and growth of carbamide, a molecular crystalline material [18,19]. However, studies on its dissolution in water when used as a space holder in the production of metallic porous structures have been limited by the amount of carbamide dissolved. Therefore, this study is a pioneering kinetic study of the dissolution of carbamide within raw porous structures before sintering. Depending on the properties of the porous medium, such as size, shape, ratio, and whether the pores are open or closed, the solution flowing through the pores can vary significantly, affecting the dissolution rate. Carbamide is an organic compound with the chemical formula $(NH_2)_2CO$. It hydrolyzes uncharged carbamide into charged ammonium and bicarbonate ions, increasing the overall conductivity of a solution, as shown below in Eq. (1) [19,20]. Conductometry has become an alternative and promising method for determining the dissolution rate of carbamide in water, where it is used as a space holder in porous structures [21].

$$NH_2CONH_2 + 3H_2O \rightarrow 2NH_4^+ + HCO_3^- + OH^- \quad (1)$$

In the production of porous metallic materials, the controlled removal of space holders plays a decisive role in determining the final pore morphology, distribution, and mechanical integrity of the structure. The release profile and rate of space holders, such as carbamide, are among the most critical parameters affecting the uniformity and functionality of the pores formed. Any uncontrolled or incomplete removal may lead to pore collapse, non-uniform distribution, or residual contamination, ultimately compromising the desired properties of the porous material. Therefore, understanding the dissolution behavior of carbamide in aqueous media and modelling its release kinetics is essential for optimizing the space holder removal process. This study contributes to the evaluation of critical quality attributes of green compacts by understanding the space holder dissolution process in porous formation. This study was conducted to address this need by systematically examining the aqueous leaching of carbamide through conductometric analysis and developing a kinetic model to support the controlled and reproducible fabrication of porous structures. This study is original in that it combines conductometric analysis with kinetic modelling to quantitatively monitor the aqueous dissolution behavior of carbamide as a space holder. The study provides original and quantitative data on the dissolution process of carbamide, contributing to a better understanding of the dissolution mechanisms of similar compounds. Furthermore, it highlights the potential of conductometric analysis as an effective tool for kinetic studies in such systems.

2. Experimental procedures

2.1. Materials

Low alloy steel foams were produced by the space holder-water leaching technique in powder metallurgy, employing pre-alloyed Cu-Ni-Mo steel powders (Distaloy AB), which are water-atomized and commercially produced by Höganäs Company, Sweden. The powder composition consisted of 1.5 wt% Cu, 1.75 wt% Ni, 0.5 wt% Mo, with the remainder being Fe. Carbamide particles were selected as space holder to create the porosity in the steel foam samples because it easily

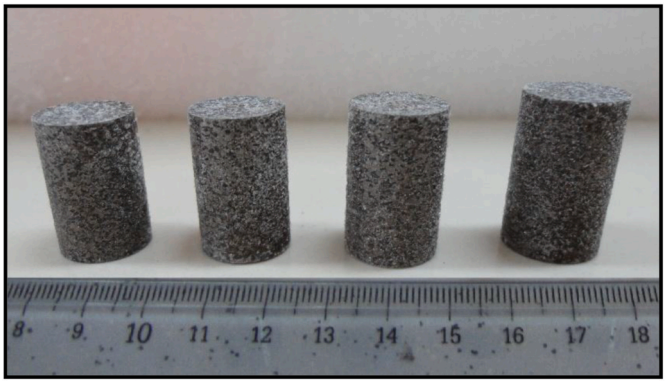

Fig. 1. Photograph of the green specimens having different carbamide volume fractions.

evaporates at a very low temperature under an air atmosphere as mentioned in the previous section. It was procured purity>99.5% from Merck, Germany. These particles exhibited a density of 1.34 g/cm^3, a melting point of 133 °C, and a water solubility exceeding 1000 g/L at 20 °C. Spherical carbamide particles were sieved to isolate the −1400 + 1000 μm size range. Additionally, the spherical particles were mechanically crushed to produce non-spherical carbamide, which was then sieved to obtain the same −1400 + 1000 μm size fraction. The polyvinly-alcohol solution (97.5 wt% distilled water and 2.5 wt% PVA) was used as binder (PVA supplied by Merck, Germany) to prevent the raw compact samples from disintegrating during dissolution and to ensure mechanical strength before sintering. Scanning electron microscope (SEM) analysis of the Distaloy AB steel powder and carbamide particles with different shapes were obtained using a JEOL JMS 5600 scanning electron microscope. The size distributions of pre-alloyed steel powders were performed in a Malvern Mastersizer 2000 device operating on the principle of laser light diffraction measurements. In order to investigate the weight change of carbamide with increasing temperature, thermogravimetric/differential thermal analysis (TG/DTA) analysis was performed under a nitrogen atmosphere using a TA Instruments SDT Q600 device at a constant heating rate of 5 °C/min.

2.2. The process of coated carbamide with powder mixture and green compacts production

In this study, the production process of green steel foams using the carbamide particles as the space holder consisted of four main steps, excluding the sintering process of the green compacts for the steel foam production. These main steps included: (i) preparation of the mixtures containing steel powder and binder, (ii) coating process of the carbamide particles with the powder mixtures, (iii) compaction process of the coated carbamide particles, (iv) dissolving process of carbamide particles by water leaching in green compact parts. Initially, the PVA solution was incorporated at a proportion of 2 wt% relative to the mass of the steel powders. The steel powders were manually blended with PVA solution to ensure uniform distribution. In the second step, the mixing of the powder and carbamide was mixed in different volume fractions of 50, 60, 70, and 80 vol% carbamide particles in a Turbula type mixer for 60 min. These values constitute the theoretical porosity value. Theoretical porosity is the porosity calculated from the initial ratios of space-holder and metallic powders; it includes all pores, both open and closed. The amount of carbamide to be added to 10 g of metal powders to prepare samples containing pores at the targeted ratios was calculated using the relationship given in Eq. (2).

$$m_k = \frac{10.G_n.\rho_k}{(100 - G_n).\rho_t} \tag{2}$$

Here, m_k is the amount of carbamide to be added in the mix (g), Gn is the target porosity in the samples (by volume, %), ρ_k is the density of carbamide (1.34 g/cm^3), and ρ_t is the theoretical density of steel powder (2.7 g/cm^3).Before the mixing process, all the powder was treated with 0.75 ml of ethanol to prevent segregation of steel powders and carbamide particles. Imaging of coated carbamide particles with steel powders was performed under a stereomicroscope (Nikon ME600). In the third step, the coated carbamide particles with powder mixing were then compacted at 200 MPa into cylindrical shapes with a 12 mm diameter and height of about 18 mm using a die made of H13 tool steel (DIN 1.2344) by a hydraulic press machine (Apex, 6000 kg capacity). Fig. 1 shows the photograph of the green specimens after compacting. Finally, the green specimens containing different proportions and shapes of carbamide were immersed in distilled water at room temperature to leach the carbamide.



Fig. 2. Process of monitoring carbamide dissolution with conductometer.

2.3. Dissolution process of carbamide and conductivity measurement

Due to the absence of metallurgical bonding before sintering, the green compacts possessed relatively low mechanical strength, which primarily depended on the applied compaction pressure. The appropriate press pressure was determined in a previous study [7]. During the leaching experiments, the specimens were carefully handled and immersed in the water bath on a glass substrate to minimize mechanical disturbance during conductivity measurements. No additional fixtures or protective equipment were employed throughout the experimental procedure. Green compacts were immersed in distilled water at 25 °C for different times until fully dissolved, depending on the carbamide content, to remove carbamide particles. The amount of dissolved carbamide in the specimens was determined using a Jenco 6350 PH/COND/TEM conductivity meter. The analysis was based on changes in the electrical conductivity of the solution, a process originally developed by Chin and Kroontje [17]. The conductivity meter, which measures the amount of electric current in a solution, consists of a power source, a conductivity cell containing the test solution, and a resistance measurement unit. The conductivity cell is equipped with platinum electrodes coated with platinum black. The device automatically applies temperature compensation and reports conductivity values as if measured at 25 °C. Before measurements, the instrument was calibrated using a potassium chloride (KCl) solution with a known conductivity. After the probe is placed in a container filled with pure water containing the raw carbamide-containing sample to be dissolved, the measuring device applies a voltage between two electrodes inside the probe. The electrical resistance of the solution causes a voltage drop, which is read by the measuring device. The measuring device converts this reading to

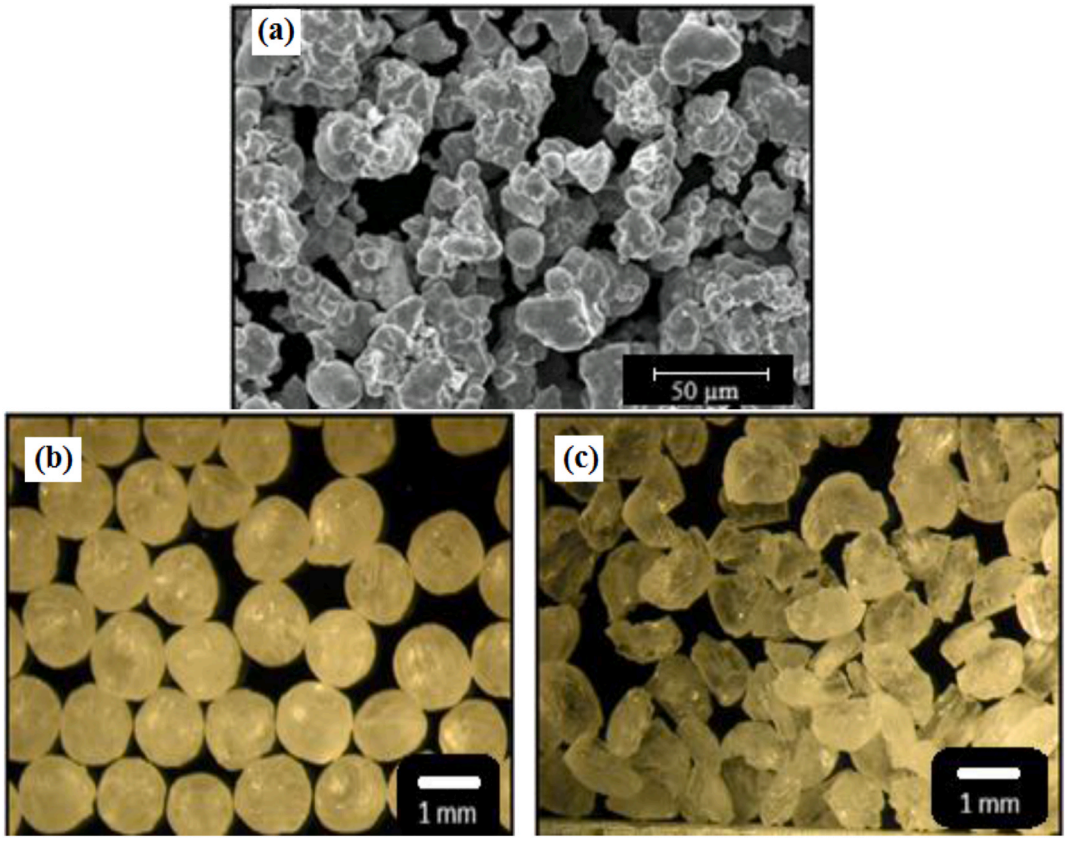

Fig. 3. Typical morphologies of raw materials: a) water atomized steel powder, b) spherical shaped carbamide particles, and c) non-spherical carbamide particles.

micro-Siemens per centimeter. This value indicates the total amount of dissolved carbamide. The total amount of dissolved carbamide is the amount of solid material dissolved from the green specimens after pressing. Standard carbamide solutions with concentrations of 0.15, 0.3, 0.5, 0.8, 1.0, 1.5, 2.0, 2.5, 3.0, 4.0, 5.0, 7.5, and 10.0 M were prepared by dissolving carbamide in deionized water, and their conductivities were measured. All the measurements were conducted in triplicate at ambient conditions. Subsequently, green samples containing different amounts and shapes of carbamide were immersed in a deionized water bath. The deionized water molecule is resistant to electricity. As the impurities in water increase, its conductivity increases. By measuring water conductivity, the amount of impurities coming from dissolved carbamide is determined. The conductivity of the solution was recorded at specific time intervals. The corresponding amount of dissolved carbamide during the leaching process was then determined by comparing the measured conductivity values with the conductivity–carbamide concentration relationship established from the standard solutions. Fig. 2 shows the experimental setup used to measure the conductivity during the dissolution process of carbamide.

2.4. Kinetic study

In this study, the leaching kinetics of carbamide from carbamide and metal powder compacts at different ratios were also investigated. A model-based analysis of the dissolution behavior of compacts was used. Zero-order, First-order, Second-order, and Korsmeyer-Peppas kinetic models were used for the investigation of the dissolution behavior of the carbamide and metal powder compacts. The following formulations were applied for this investigation.

- Zero-order equation:

$$Q_t = Q_0 + k_0 t \tag{3}$$

- First-order equation:

$$log\ Q_t = log\ Q_0 - \frac{k_1 t}{2.303} \tag{4}$$

- Second-order equation:

$$\frac{1}{Q_t} = \frac{1}{k_2 Q_0^2} + \frac{t}{Q_0} \tag{5}$$

- Korsmeyer-Peppas equation:

$$F = \frac{M_t}{M_\infty} = k_{kp} t^n \tag{6}$$

Here, Q_0 (ppm) and Q_t (ppm) indicate the cumulative carbamide release at the initial time ($t = 0$) and at a given time t, respectively. The constants k_0 ($ppm \cdot h^{-1}$), k_1 (h^{-1}), k_2 ($ppm^{-1} \cdot h^{-1}$), and k_{kp} (h^{-n}) correspond to the release rate parameters for Zero-order, First-order, Second-order, and Korsmeyer–Peppas models. F represents the fraction of carbamide released into the medium at time t, determined as the ratio of M_t (amount of carbamide released at time t) to M_∞ (maximum release at infinite time). The exponent n is the diffusion constant that characterizes the transport mechanism driving the release. Distinct values of n indicate different mechanisms: $n \leq 0.43$ reflects Fickian or quasi-Fickian diffusion, $0.43 < n < 0.89$ implies non-Fickian diffusion associated with anomalous release behavior, $n = 0.89$ corresponds to zero-order (relaxational) transport, and $n > 0.89$ is indicative of super case II transport [22–27].

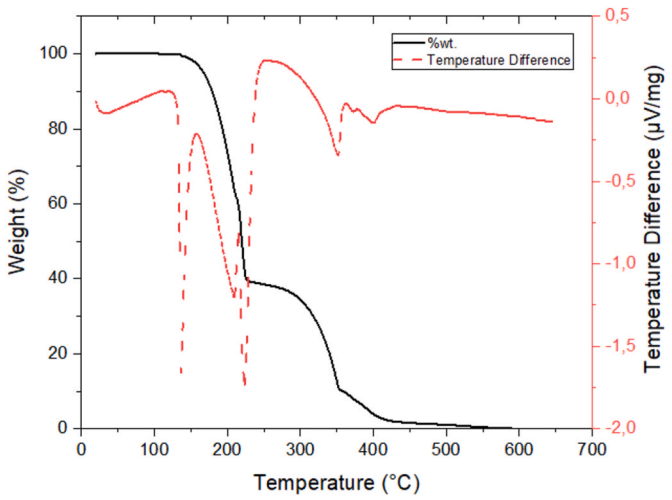

Fig. 4. TG/DTA analysis results of carbamide.

3. Results and discussion

3.1. Characterization results of metal powders and carbamide particles

SEM images of pre-alloyed steel powders and stereo microscopic images of different shaped carbamide particles are presented in Fig. 3. The image in Fig. 3(a) shows the morphology of the steel powders. The particles appear irregularly shaped with a partially rounded structure and a rough surface texture. The steel powders exhibited a particle size distribution ranging from 45 μm to 150 μm, with an average particle diameter of approximately 109 μm. The particles displayed a generally rounded morphology with slight irregularities. This morphology is typical of water-atomized powders, which enhances mechanical interlocking and compressibility during compaction processes. The particle size distribution appears relatively uniform. Fig. 3(b) depicts spherical-shaped carbamide particles. These particles exhibit a smooth, uniform surface and near-perfect spherical geometry. The spherical shape is advantageous in promoting uniform flow behavior and homogeneous pore distribution when used as a space holder in porous material synthesis (e.g., metallic foams) [7,28]. Fig. 3(c) presents the non-spherical carbamide particles. These particles show a wide variation in size and geometry, with angular and broken edges. The irregular morphology can lead to non-uniform packing density and a more random pore architecture when used as a space holder. While this may reduce the control over final porosity distribution, it can be useful when stochastic or gradient pore structures are desired in functional applications such as filtration or catalysis [29–32].

The thermal decomposition behavior of carbamide was investigated by simultaneous thermogravimetric analysis and differential thermal analysis, and the results are presented in Fig. 4. The TG curve (black line) shows the weight loss profile of carbamide as a function of temperature, while the DTA curve (red dashed line) indicates the thermal events accompanying this degradation. The initial mass remained stable up to approximately 150 °C, indicating thermal stability in this range. The first major decomposition stage occurred between 150 °C and 220 °C, where a rapid mass loss of approximately 60% was observed in the TG curve. This significant weight reduction is mainly attributed to the primary thermal decomposition and volatilization of carbamide, involving the release of gaseous products such as ammonia (NH_3) and isocyanic acid (HNCO). The sharp thermal event observed in the DTA curve within this region further confirms the intense decomposition reactions occurring after melting. Between 220 °C and 270 °C, the TG curve exhibited a relatively slower mass loss of approximately 5%. This stage is associated with the formation and partial decomposition of intermediate compounds such as biuret, cyanuric acid, and triuret generated during the decomposition process. Subsequently, another

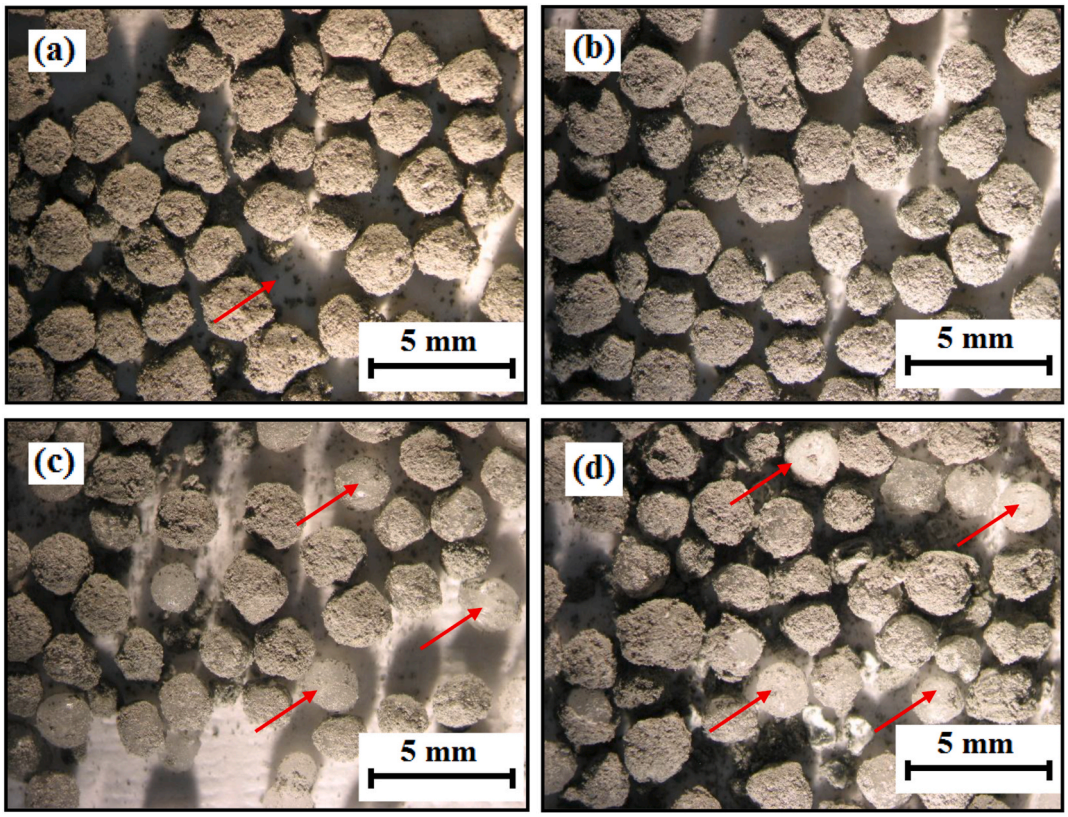

Fig. 5. Photograph of coated spherical shaped carbamides: a)50 vol%, b)60 vol%, c)70 vol%, and d)80 vol% carbamide particles.

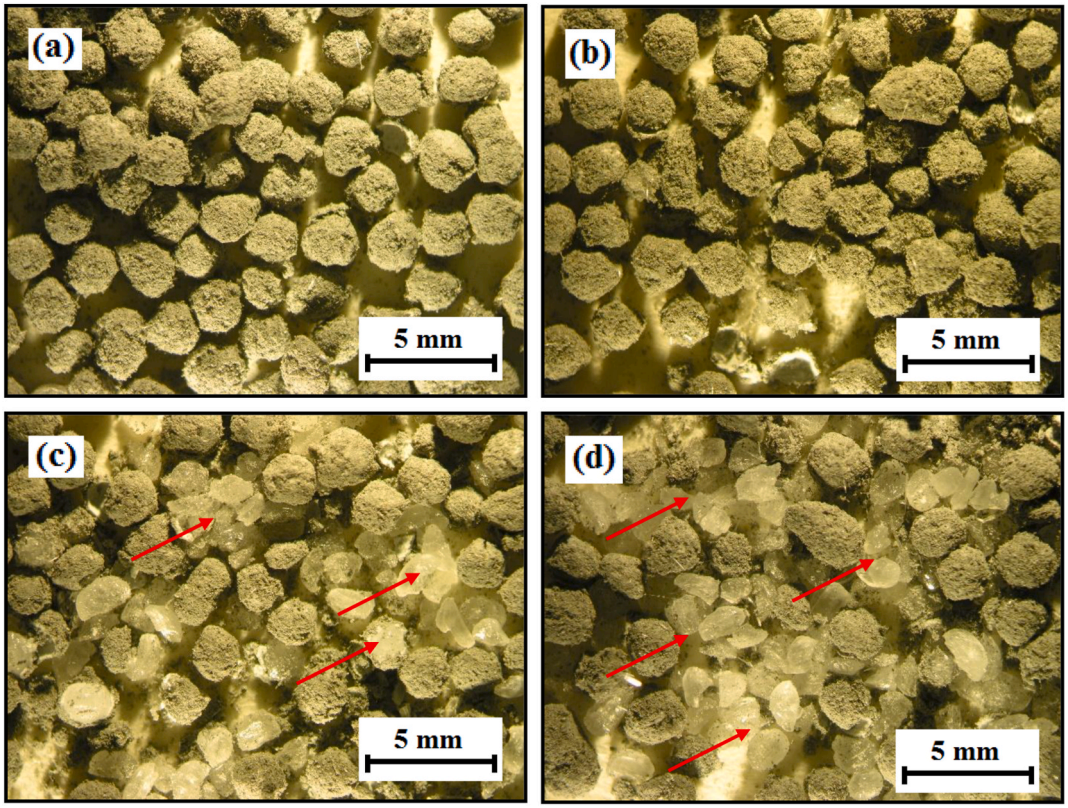

Fig. 6. Photograph of coated non-spherical carbamides: a) 50 vol%, b) 60 vol%, c) 70 vol%, and d) 80 vol% carbamide particles.

rapid weight loss was observed between 270 °C and 350 °C, where the remaining mass decreased from approximately 35% to nearly 10%. This stage corresponds to the further degradation and volatilization of the previously formed intermediate species. Beyond 350 °C, the TG curve gradually approached a plateau, while the DTA signal became stable, indicating that the thermal decomposition process was nearly complete. The total mass loss exceeded 90%, demonstrating that carbamide is almost entirely converted into volatile decomposition products with minimal solid residue remaining after heating. The obtained results confirm that carbamide undergoes a multi-step thermal degradation process characterized by distinct endothermic transitions and substantial mass loss. Such behavior highlights its suitability as a space-holder material for porous metal production processes requiring controlled decomposition and gas release. It has been reported in many studies that the main limitation of carbamide removal by thermal evaporation is its low economic efficiency, since crack-free porous structures generally require very slow heating rates. Moreover, the decomposition process is time-consuming and may release environmentally harmful gases during heating [14,29,31,33,34]. Due to the drawbacks of the evaporation technique, leachable techniques using space holders used in this study are considered an attractive and environmentally friendly method as it does not cause any hazardous by-products or emissions and does not create any toxicity [7,10,29–31,33–35].

3.2. Observation results of coated carbamide particles with different shapes

Coating the carbamide surface with steel powders is the primary objective of the mixing process. The mixing process is crucial in the production of porous metal structures using the space holder-water leaching technique in powder metallurgy. Varying the space holder morphology and ratio alters the mix quality, which in turn alters the coating uniformity of the space holder surface [30,31,33,36]. This study visually examines the coated carbamide particles having different amounts and shapes with the steel powders, and an attempt was made to establish a connection between the coating uniformity of the carbamide surface and the dissolution process.

Fig. 5 displays the photographic images for porosity level of 50 vol%, 60 vol%, 70 vol% and 80 vol% coated spherical shaped carbamide particles with steel powder mixture after the final mixing. These images were captured to qualitatively evaluate the coating homogeneity and powder coverage on the surface of carbamide particles used as a space holder. At theoretical porosity of 50 vol%, the spherical carbamide particles appear partially coated. While the spherical shape is well-defined, the surface coating is not completely uniform. In some areas, excess metal powder remains unable to cover the carbamide surface. This visible phenomenon results in the presence of thinner metal powder layers. This suggests that sufficient powder is present to form a continuous coating, which could affect blank strength and pore connectivity during sintering. At theoretical porosity of 60 vol%, the spherical carbamide particles are almost completely and uniformly coated. The texture of the coated surfaces is more uniform, and the metal powders form a dense, continuous shell around the spherical core. This ratio provides an optimal balance for maintaining good coating integrity while maintaining the round shape of the space holder. Compared to theoretical porosity of 50 vol%, a noticeable improvement in metal particle distribution and adhesion is observed, resulting in better inter-particle bonding. Theoretically, the spherical carbamide particles cannot be fully coated due to insufficient metal powder ratio in the theoretical porosity of 70 vol% condition. This situation became more pronounced at a theoretical porosity of 80 vol% due to the increased carbamide surface area and decreased metal powder content. Fig. 5(c and d) show carbamide surfaces not coated with metal powders, indicated by arrows. This is due to insufficient metal powder, which leads to the formation of thin pore walls between the pores in the final product. This also affects packing uniformity and can lead to irregular pore structures from uncoated space holders after the space holders is removed. Bekoz and Oktay [10], Jain et al. [29] and Hsu et al. [37]

reported that the contact between the steel powders and carbamide particles decreases with decreasing space holder size at higher fractions. They noted that with irregular morphologies and the use of high fraction carbamide, the total surface area of the space holder is larger, making complete coating more difficult.

Fig. 6 also presents the photographic images for porosity level of 50 vol%, 60 vol%, 70 vol% and 80 vol% coated non-spherical carbamide particles with steel powder mixture. At theoretical porosity of 50 vol%, metal powders coated the irregularly shaped carbamide surfaces, with the excess dispersed among the particles. As the theoretical porosity increases to 60 vol%, a noticeable improvement in coverage is observed. Most carbamide surfaces appear well-coated, although some gaps and thinner regions still exist. The non-spherical shape of the particles continues to present challenges for uniform powder adhesion, but the coating is more continuous compared to theoretical porosity of 50 vol% case. At theoretical porosity of 70 vol%, most of the non-spherical carbamide particles are densely and uniformly coated. Metal powder is insufficient to effectively fill the surface valleys and adheres to sharp edges, enhancing particle encapsulation. With theoretical porosity of 80 vol%, a significant number of uncoated or loosely bound carbamide particles become visible. Fig. 6(c and d) show carbamide surfaces not coated with metal powders, indicated by arrows. The irregular surface structure of the carbamide particles results in increased surface area, which makes it more difficult to coat compared to spherical particles. Due to the angular geometry and high surface roughness of the carbamide particles, certain regions remain partially exposed. This incomplete coverage may result in weaker interfacial bonding and non-uniform porosity development after space holder removal. The excessive metal powder content likely leads to poor dispersion and partial agglomeration, reducing coating uniformity. Additionally, free metal particles may bridge between non-spherical carbamide particles, introducing packing irregularities and potentially affecting porosity uniformity in the final structure. At equivalent metal powder contents, spherical particles show higher coating efficiency and fewer tendencies for particle agglomeration. Metal powders adhere well to the smooth surfaces and do not easily bridge between neighboring spheres, maintaining discrete coated units. Jain et al. [33] and Sazegaran et al. [31] reported that the coating uniformity of the space holder is affected by the particle size and volume fraction of carbamide. It was emphasized that a decrease in the carbamide content in the mixture increases the contact rate between the steel powder particles, while a increase in the carbamide content results in the formation of uncoated carbamide. Observations in the present study indicated that the quantity of carbamide particles among the steel powder-space holder particles determines the quality of the mixture more than the shape of the carbamide. Optimum coating uniformity was observed in mixtures containing 60 vol% carbamide particles of spherical and irregular shapes.

3.3. Dissolution process of carbamide particles by water leaching in green compacts

Many studies have emphasized that the performance of metal foams depends particularly on the foam's manufacturing process [4,14,32,38]. The methods of space holder removal during the manufacturing process also have a significant impact on these foam structure properties. The widespread use and successful application of steel foams necessitate a detailed understanding of these processes. In the case of complete or relatively dense metal-powder coverage, water penetration toward the carbamide particles is expected to be slower because the dissolution medium must pass through the microscale gaps and interparticle channels within the metal-powder layer. Nevertheless, these microscale gaps provide pathways through which water penetrates through microscale gaps and reaches the carbamide surface. When carbamide begins to dissolve in water, water molecules surround the carbamide molecules, breaking the intermolecular forces that hold the carbamide together in a solid state, initiating the dissolution process. Once wetted, the carbamide dissolves and the resulting dissolution further enlarges the available pathways, facilitating the transport of dissolved carbamide toward the external surface. Water conductivity is one of its most important properties. Pure water molecules do not conduct electricity, but as carbamide dissolves, impurities in the water increase, increasing its conductivity. Measuring water conductivity provides an idea of the amount of carbamide present in the raw material and the dissolved product. Stefanoni et al. [39] reported that the dissolution rate of space holders is highly dependent on both the porosity and dissolution conditions of the porous medium surrounding the steel. However, this phenomenon is difficult to explain because the mechanism controlling dissolution rates in porous materials is not fully understood [39]. This study analyzes the dissolution rate of space holders, in green compacts containing different space-holder shapes and volume fractions.

In this study, the dissolution behavior of spherical and non-spherical carbamides in green compacts (coded as S and NS, respectively) were evaluated across four distinct porosity levels for porosity level of 50 vol %, 60 vol%, 70 vol% and 80 vol%. The leaching process of carbamide was performed without any distortion or deformation of the green samples. The amount and shape of carbamide particles affected removal process. The experimental data were fitted to four commonly used kinetic models: zero-order, first-order, second-order, and the Korsmeyer–Peppas (KP) empirical model. The evaluation focused on comparing the goodness of fit (R^2) for each model under each condition to determine the most suitable kinetic description, while considering the impact of porosity on the underlying release mechanism. Sipponen et al. [40] stated that the carbamide release process involves dissolution and water penetration into the material and that leaching kinetics can be simplified to a diffusion process according to Fick's second law of diffusion. They reported that diffusion is a measure of solute retention within a solid matrix and can be used to predict carbamide release for different particle sizes and geometries. The leaching kinetics obtained in this study provide important insights into the optimization of porous metal fabrication processes, particularly for powder metallurgy routes employing carbamide as a space holder. The dissolution behavior directly affects the efficiency of pore former removal, which subsequently influences the homogeneity, interconnectivity, and integrity of the resulting porous structure. Incomplete or non-uniform carbamide removal may lead to residual contaminants, localized densification, or irregular pore morphology, thereby adversely affecting the mechanical stability and functional performance of the produced porous metals. In contrast, controlled and efficient dissolution promotes the formation of interconnected pore networks that are essential for applications requiring lightweight structures, energy absorption, permeability, or biomedical compatibility. The findings of the present study can also be associated with our previous work [14], where carbamide removal results based on leaching and thermal evaporation routes were comparatively investigated. The previous study demonstrated that the removal technique significantly influences pore morphology, dimensional stability, and defect formation within porous metallic structures. In particular, rapid or incomplete removal conditions were shown to increase the risk of pore collapse and structural heterogeneity, whereas controlled dissolution promoted more uniform and interconnected porosity. In this context, the current kinetic analysis contributes to a deeper understanding of the dissolution-controlled pore formation mechanism and provides valuable guidance for selecting appropriate processing parameters such as carbamide content, carbamide shape, dissolution duration, and removal method. In conclusion, understanding the kinetics of the pore-forming agent's removal from the medium directly impacts the manufacturing process. If the reaction proceeds faster or slower than it should, pore formation within the structure cannot be fully understood. This leads to manufacturing defects such as unwanted voids, weak pore wall connections, or brittleness, reducing the mechanical strength of raw samples before sintering. To minimize these defects in the manufacturing process, accurate optimization of

Table 1
Comparison of kinetic models for carbamide dissolution.

	Carbamide fraction (vol%)	*Zero Order*		*First Order*		*Second Order*		*Korsmeyer-Peppas*		
		k	R^2	K	R^2	k	R^2	k	R^2	n
Spherical	**50%**	0,0635	0,9078	0,001381800	0,9786	0,000018686	**0,9925**	0,952311492	0,9617	0,65
	60%	0,1125	0,9370	0,002763600	**0,9924**	0,000010507	0,9721	0,567343592	0,9771	0,77
	70%	0,2201	0,9485	0,006678700	**0,9847**	0,000009796	0,9345	0,705717758	0,9805	0,83
	80%	0,3648	0,8994	0,014278600	**0,9776**	0,000017884	0,8744	1,478921829	0,9711	0,80
Non-Spherical	**50%**	0,0746	0,9127	0,001612100	0,9693	0,000016039	**0,9795**	0,831707319	0,9646	0,68
	60%	0,1346	0,8519	0,003684800	**0,9503**	0,000010611	0,8146	0,556647699	0,9463	0,81
	70%	0,3214	0,8885	0,012896800	**0,9842**	0,000020384	0,9005	1,614840612	0,9679	0,78
	80%	0,5822	0,8858	0,035466200	0,9189	0,000023127	0,8184	2,329164162	**0,9655**	0,81

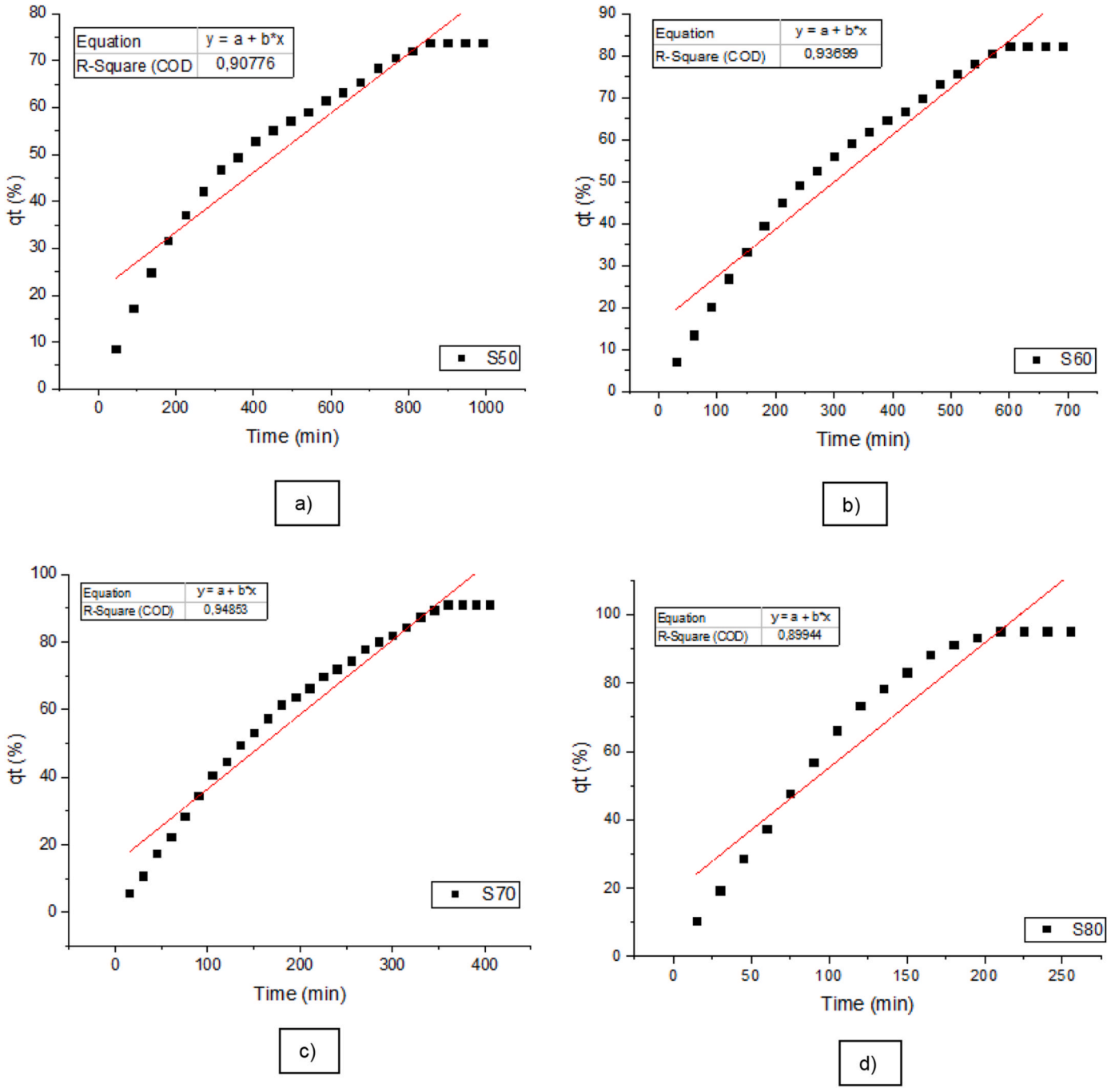

Fig. 7. Zero-order kinetics of spherical samples a) S50, b) S60, c) S70, and d) S80.

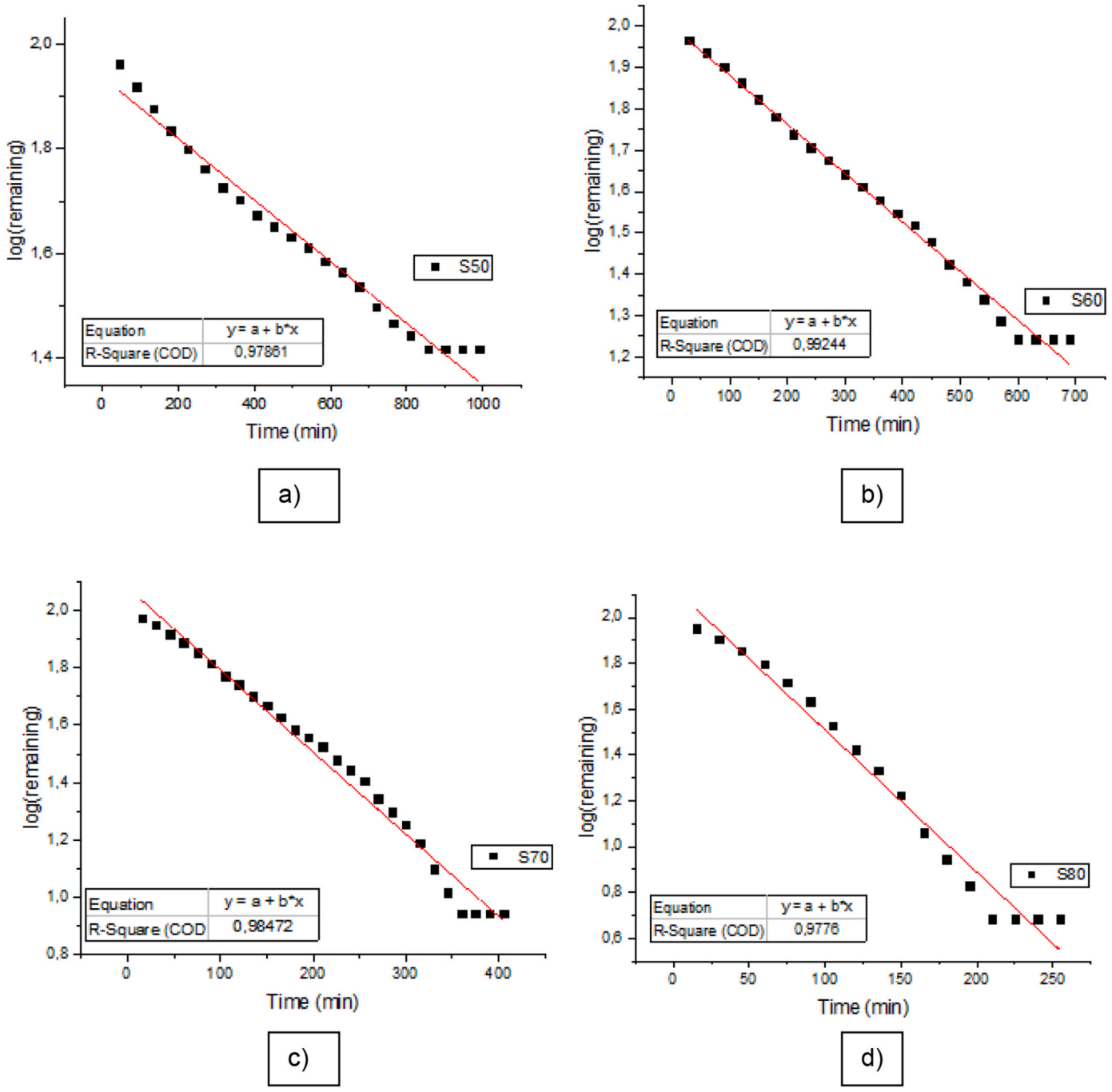

Fig. 8. First-order kinetics of spherical samples a) S50, b) S60, c) S70, and d) S80.

kinetic data is necessary.

The results obtained from kinetic studies are given in Table 1 and Figs. 7–14. Both S and NS coded samples at theoretical porosity of 50 vol % showed the best fit with the second-order kinetic model, with R^2 values of 0.9925 and 0.9795, respectively. This suggests that at low porosity, the dissolution process is governed by a rate dependent on the square of the remaining carbamide concentration. Such behavior is consistent with earlier findings for compacted carbamide formulations, where dissolution at low porosity is often influenced by limited solvent penetration and high concentration gradients within the porous structure [22]. The relatively poor fit of the zero-order model ($R^2 < 0.92$) in both samples further supports the view that dissolution is not proceeding at a constant rate but rather is dynamically controlled by reactant availability.

As porosity increased for porosity level of 60% and 70 vol%, the leaching behavior increasingly followed first-order kinetics. In these conditions, the dissolution rate appeared proportional to the remaining carbamide concentration, with R^2 values exceeding 0.98 in most cases. This transition reflects a structural shift wherein increased pore volume facilitates solvent ingress and enables a more homogenous concentration gradient throughout the green specimens. These observations are in line with prior work on porous nutrient carriers and controlled-release fertilizers, where first-order models frequently described systems with sufficient permeability to sustain diffusion-limited release [23,24]. The good agreement with first-order kinetics under these conditions implies that mass transfer within the samples was less obstructed and primarily governed by the intrinsic solubility dynamics of carbamide.

At the highest porosity level of 80 vol%, divergence emerged

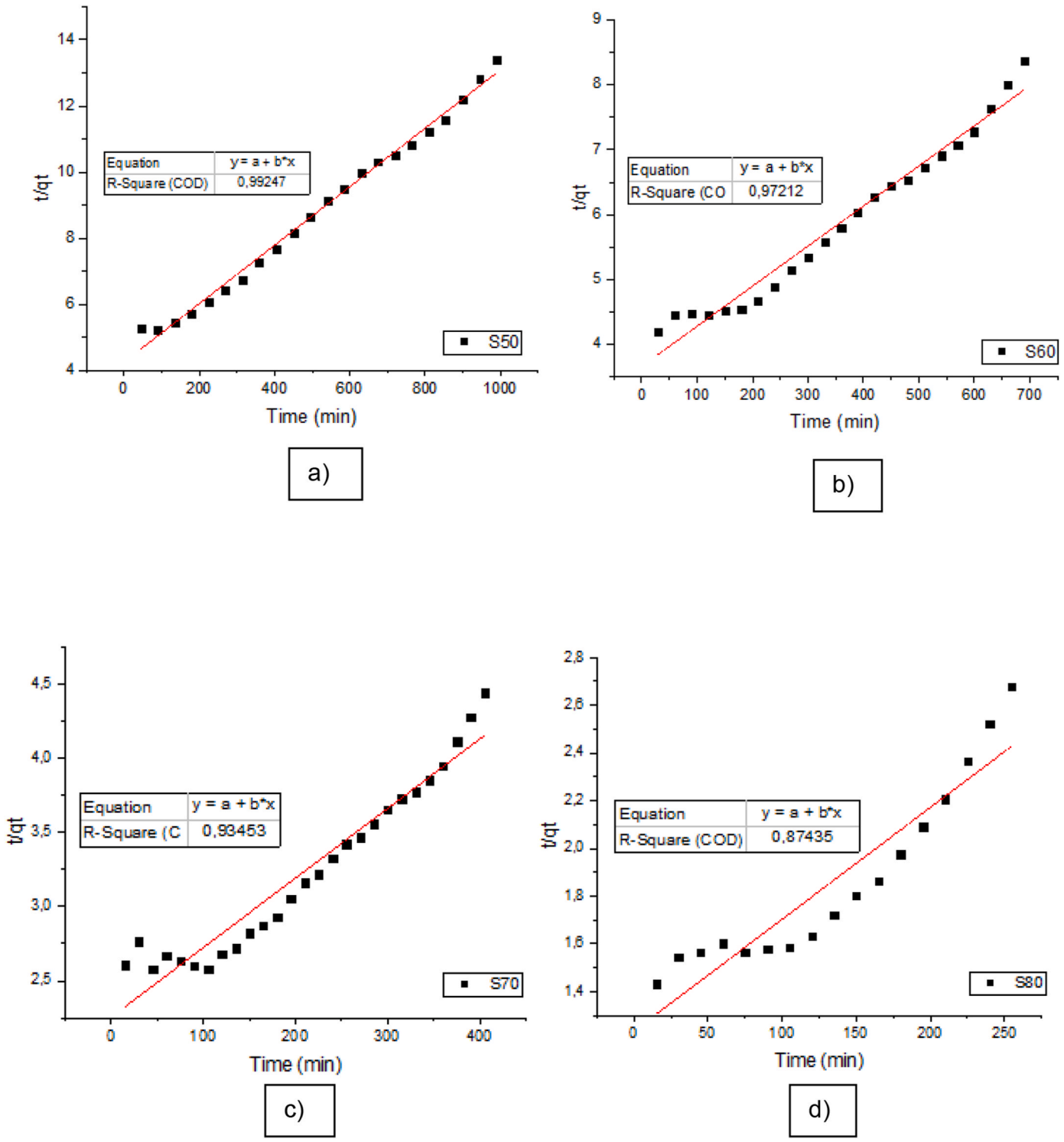

Fig. 9. Second-order kinetics of spherical samples a) S50, b) S60, c) S70, and d) S80.

between the two sample types. For the S sample, the first-order model continued to provide the best fit ($R^2 = 0.9776$), maintaining a consistent dissolution profile across porosities. However, the NS sample displayed a shift in kinetic preference, with the KP model offering the highest R^2 value (0.9655), surpassing both first-order and second-order fits. This shift suggests a change in the dominant leaching mechanism, indicating that, in addition to diffusion, solvent transport through interconnected pore channels and mass transfer within the porous structure contribute to the overall carbamide leaching behavior. The KP model, widely applied in describing drug and nutrient release from polymeric or porous matrices, accounts for anomalous transport behavior by integrating both Fickian diffusion and non-Fickian mechanisms such as structural rearrangement [25,26]. The stronger performance of the KP model in the NS-80 vol% sample indicates that the release mechanism may no longer be purely diffusion-controlled, particularly when the internal pore network is advanced.

The n values obtained from the KP model ranged between 0.45 and 0.89 for all samples and porosity conditions. These values fall within the

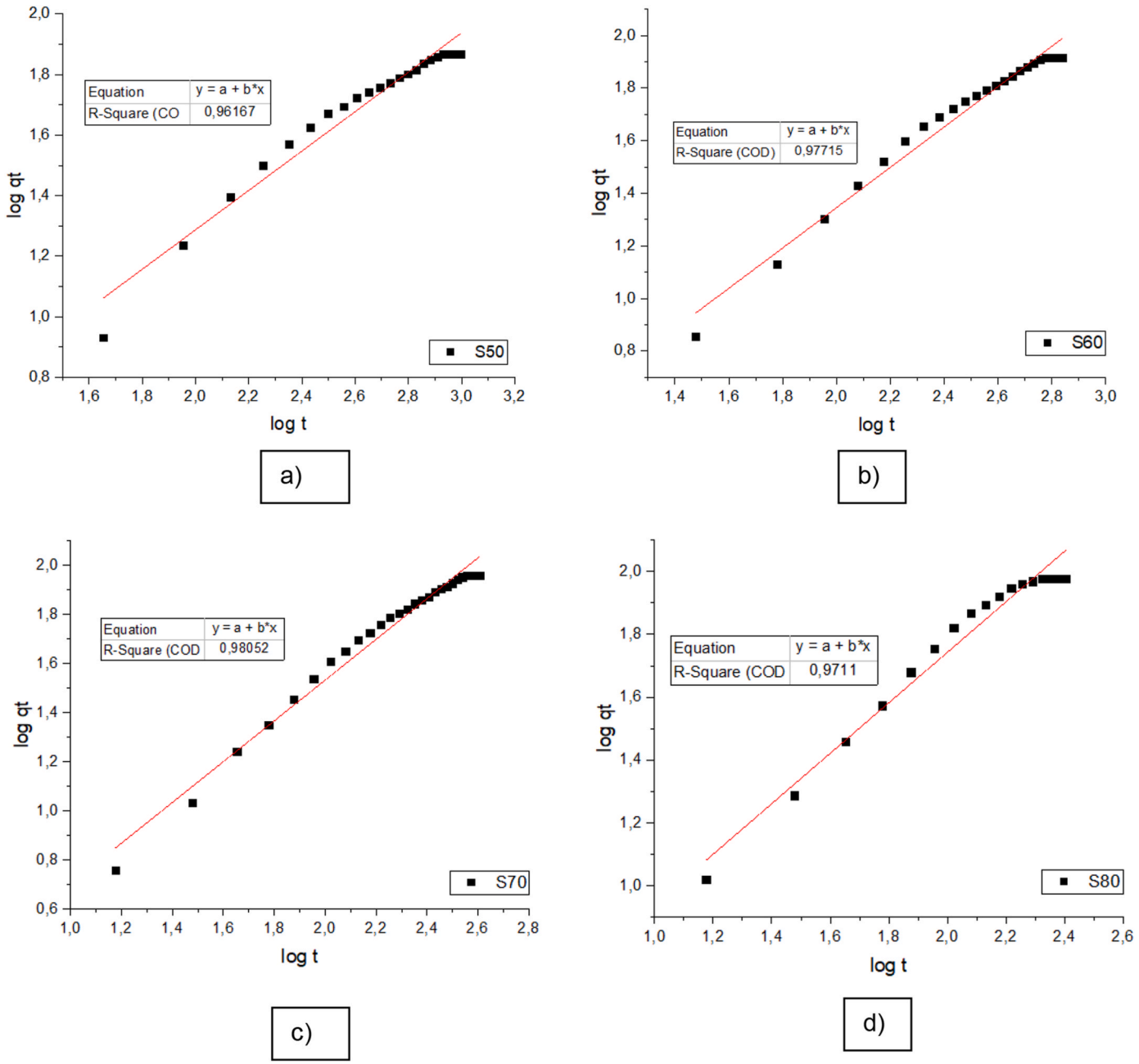

Fig. 10. Korsmeyer-Peppas kinetics of spherical samples a) S50, b) S60, c) S70, and d) S80.

range characteristic of anomalous non-Fickian transport, suggesting that the leaching behavior is influenced not only by diffusion but also by solvent transport and mass transfer through the interconnected pore structure [41]. While the KP model only exhibited the highest R^2 value in one case (NS at 80 vol% porosity), the elevated n values across other samples imply that even when not the best-fitting model statistically, KP still provides valuable insight into the multi-mechanistic nature of the dissolution process. However, n values should be interpreted with caution when the KP model is not the optimal fit [42]. Nonetheless, their consistent elevation suggests that deviations from pure Fickian behavior are present in both materials.

When N and S coded samples were compared followed a similar trend of transitioning from second-order kinetics at low porosity to first-order kinetics at mid-range porosities. However, their behavior diverged at high porosity. The S sample maintained a first-order profile throughout, while the NS sample exhibited a clear shift toward complex, structure-sensitive release at 80% porosity. This difference may be attributed to intrinsic variations in microstructural properties such as pore interconnectivity, tortuosity, or physical fragility, which are known to influence leaching kinetics in porous materials [43]. These properties likely allowed the NS sample to undergo more significant particle rearrangement during dissolution, thereby increasing the relevance of non-Fickian mechanisms.

These findings are well aligned with prior studies on carbamide and slow-release materials. In particular, research by Jange et al. showed that second-order and KP models best described early-stage dissolution in compacted carbamide composites [22], while Ponnusamy et al. reported n values around 0.71 and strong KP fits for nitrogen release from mesoporous carriers [24]. Additionally, Babadi et al. demonstrated that structural modifications such as coating or high porosity led to shifts in release mechanisms, with KP behavior emerging prominently under such conditions [25]. These parallels underscore the importance of

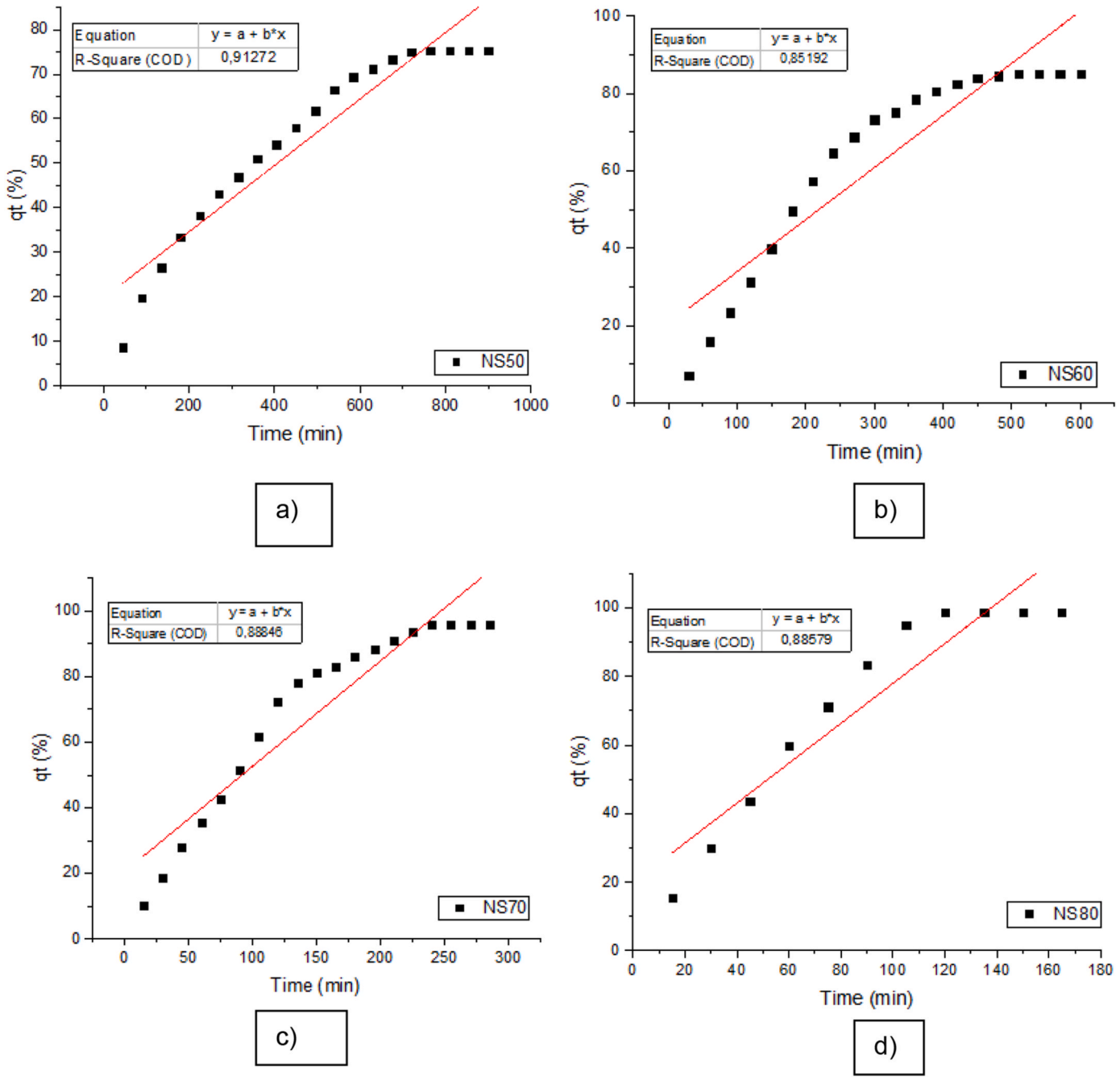

Fig. 11. Zero-order kinetics of non-spherical samples a) NS50, b) NS60, c) NS70, and d) NS80.

sample design, particularly porosity, in dictating the transport phenomena governing solute release.

In conclusion, this study demonstrates that porosity plays a pivotal role in modulating the leaching kinetics of carbamide -containing matrices. At lower porosity, limited solvent access confines the system to concentration-sensitive second-order kinetics. As porosity increases, diffusion-dominated first-order behavior emerges. At very high porosity, especially in structurally dynamic matrices such as NS, dissolution becomes increasingly influenced by anomalous transport mechanisms. The KP model provides a useful framework to capture these complexities, particularly when structural evolution during dissolution is significant. These insights offer practical implications for designing porous materials with tailored release profiles for applications. In their study on the thermodynamics of dissolution of carbamide in water, House and House [44] explained that the trends experienced during the dissolution process are due to differences in the degree of aggregation of carbamide in solvent systems.

Many studies on water-leachable space holders in powder metallurgy have reported that the shape and ratio of the space holder influence the time and temperature required during the leaching process. It has been stated that the formation of sharp, widened channels between the pores is restricted in a spherical space holder compared to an irregularly shaped space holder, which can lead to a longer leaching time [7,36,45,46]. In this study, the shape and amount of coated carbamide in green compact can determine this aggregation by affecting the coating uniformity of carbamide. It was found that amount of carbamide in the green compacts had a profound effect on the leaching time although shape of the carbamide particles were also effective.

The results of the present study indicate a direct relationship between porosity and the leaching kinetics of carbamide during water

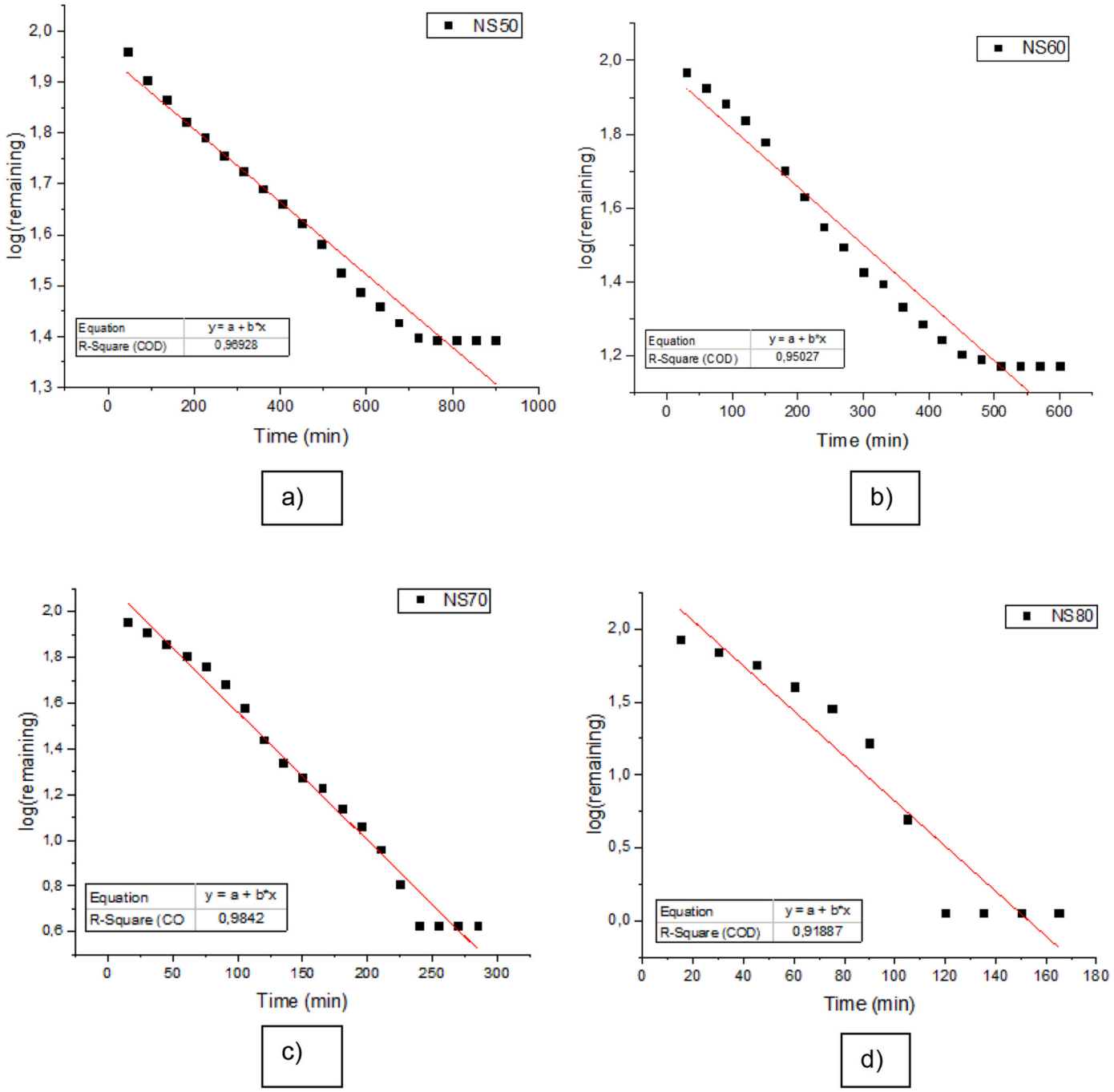

Fig. 12. First-order kinetics of non-spherical samples a) NS50, b) NS60, c) NS70, and d) NS80.

leaching. As the space holder content increases, the porosity generated during dissolution provides a larger solid–liquid interfacial area, thereby increasing the contact between water and the green compact and accelerating the dissolution process. This behavior can be explained through several interconnected mechanisms. First, a higher porosity increases the effective surface area available for solvent penetration, allowing water to access a larger fraction of the internal structure. Second, the dissolution process is predominantly governed by mass transfer and diffusion. In highly porous green compacts, the interconnected pore network facilitates solvent penetration and promotes the transport of dissolved carbamide, thereby reducing diffusion resistance and enhancing mass transfer. Furthermore, increasing the carbamide content promotes the formation of interconnected pore channels, which improve the permeability of the green compact and enable more efficient water circulation throughout the structure. Consequently, the dissolution rate increases as solvent accessibility and transport pathways improve. Kinetic analysis further demonstrated that specimens with higher carbamide contents were better described by the first-order kinetic model, whereas samples with lower porosity exhibited behavior more consistent with the second-order kinetic model. In contrast, green compacts prepared with irregularly shaped carbamide particles exhibited more heterogeneous pore networks, resulting in dissolution behavior that was more appropriately described by the Korsmeyer–Peppas model. Overall, these findings demonstrate that pore architecture, including pore volume and interconnectivity, plays a crucial role in controlling solvent transport and leaching kinetics, thereby directly influencing the efficiency of space-holder removal during the production of porous metallic materials.

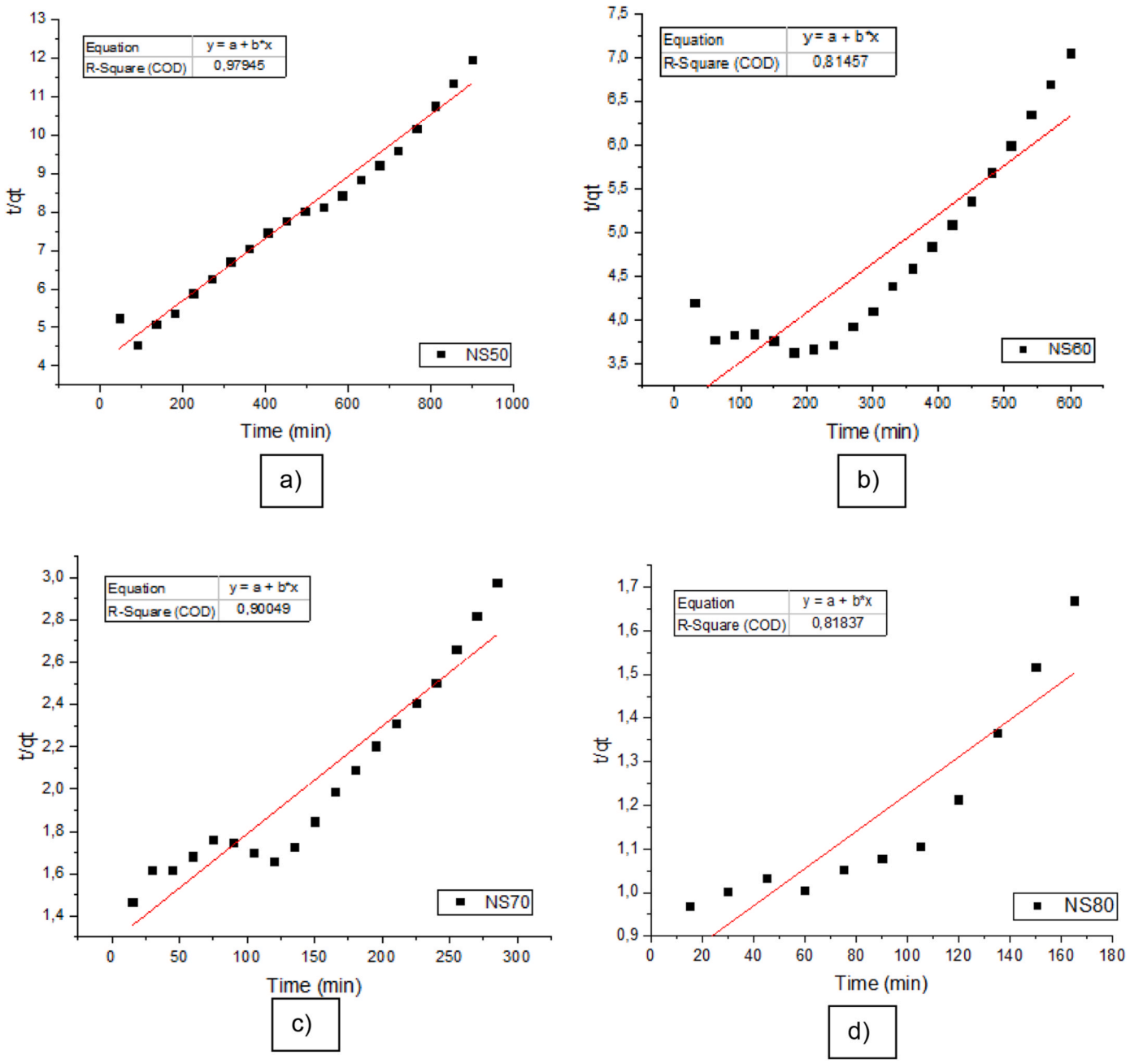

Fig. 13. Second-order kinetics of non-spherical samples a) S50, b) NS60, c) NS70, and d) NS80.

4. Conclusion

In this work, green steel foams containing the volume fraction of carbamide increase from 50% to 80%.was manufactured through powder metallurgy route using carbamide as the leachable space holder. The overall objective of this study is to evaluate the leaching process of carbamide particles with different ratios and shapes in terms of leaching kinetics and to determine the appropriate model. The results obtained could be summarized as follows.

- The macro-pores manufactured due to the dissolving of the carbamide particles were distributed in the metal matrix of the green steel foams.
- The effect of the carbamide fraction on the coating uniformity of carbamide with metal powder is dominant over the effect of the carbamide shape.
- The optimal coating for both space holder shapes was achieved in mixtures with porosity level of 60%.
- The kinetic analysis revealed a clear transition from second-order to first-order behavior as porosity increased, emphasizing a shift from interaction-controlled to diffusion-controlled dissolution.
- These findings demonstrate that understanding and controlling the dissolution behavior of the space holder are essential for achieving efficient removal and, consequently, the desired pore architecture in powder metallurgy.
- Understanding the leaching kinetics of space holders in metallic foam production provides guidance for optimizing leaching parameters, improving process control, and identifying incomplete space-holder removal that may influence the final pore architecture.

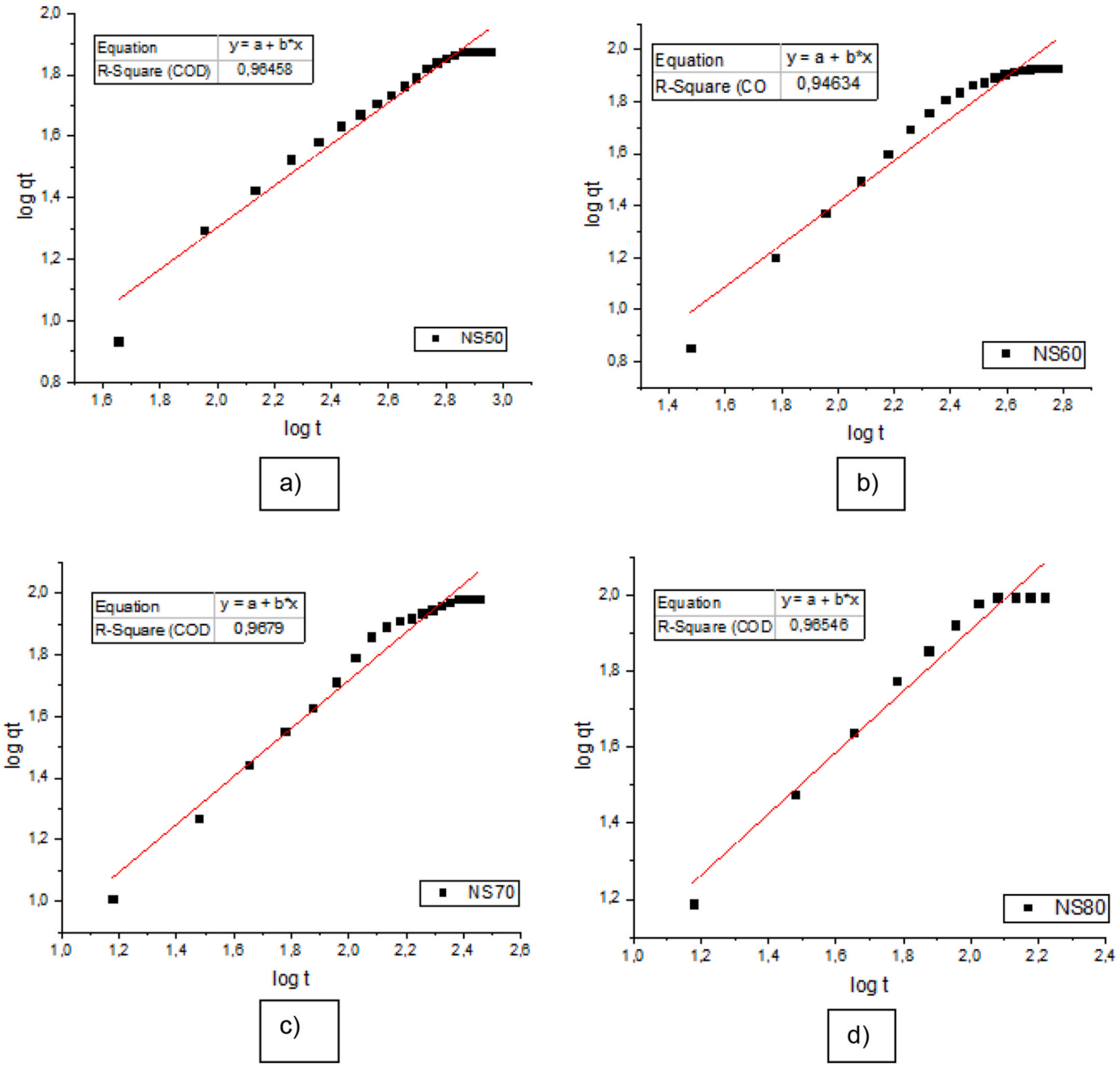

Fig. 14. Korsmeyer-Peppas kinetics of non-spherical samples a) NS50, b) NS60, c) NS70, and d) NS80.

CRediT authorship contribution statement

Nuray Beköz Üllen: Writing – original draft, Supervision, Methodology, Formal analysis. **Gizem Karabulut Şevk:** Writing – original draft, Visualization, Validation, Methodology, Formal analysis. **Ali Can Özarslan:** Writing – original draft, Visualization, Validation, Formal analysis.

Ethical approval

This study does not involve human participants or animal subjects. Therefore, ethical approval was not required.

Declaration of competing interest

The authors declare that they have no known competing financial interests or personal relationships that could have appeared to influence the work reported in this paper.

Acknowledgements

The authors have no acknowledgements to declare.

Supplementary information

No additional material was omitted from the main body of the manuscript. All relevant data and discussions necessary for understanding and reproducing the work are included within the main text to ensure clarity and readability.

Data availability

Data will be made available on request.

References

[1] M.H. Sun, S.Z. Huang, L.H. Chen, Y. Li, X.Y. Yang, Z.Y. Yuan, B.L. Su, Applications of hierarchically structured porous materials from energy storage and conversion, catalysis, photocatalysis, adsorption, separation, and sensing to biomedicine, Chem. Soc. Rev. 45 (2016) 3479–3563, https://doi.org/10.1039/C6CS00135A.

[2] A. Manonukul, N. Muenya, F. Léaux, S. Amaranan, Effects of replacing metal powder with powder space holder on metal foam produced by metal injection moulding, J. Mater. Process. Technol. 210 (2010) 529–535, https://doi.org/10.1016/J.JMATPROTEC.2009.10.016.

[3] H. Nakajima, Fabrication, properties and application of porous metals with directional pores, Prog. Mater. Sci. 52 (2007) 1091–1173, https://doi.org/10.1016/J.PMATSCI.2006.09.001.

[4] B.H. Smith, S. Szyniszewski, J.F. Hajjar, B.W. Schafer, S.R. Arwade, Steel foam for structures: a review of applications, manufacturing and material properties, J. Constr. Steel Res. 71 (2012) 1–10, https://doi.org/10.1016/J.JCSR.2011.10.028.

[5] L.-P. Lefebvre, J. Banhart, D.C. Dunand, Porous metals and metallic foams: current status and recent developments, Adv. Eng. Mater. 10 (2008) 775–787, https://doi.org/10.1002/ADEM.200800241.

[6] A. Kennedy, Porous metals and metal foams made from powders, in: Powder Metallurgy, 2012, pp. 31–46.

[7] N. Bekoz, E. Oktay, Effects of carbamide shape and content on processing and properties of steel foams, J. Mater. Process. Technol. 212 (2012) 2109–2116, https://doi.org/10.1016/J.JMATPROTEC.2012.05.015.

[8] G. Costanza, D. Solaiyappan, M.E. Tata, Properties, applications and recent developments of cellular solid materials: a review, Materials 16 (2023) 7076, https://doi.org/10.3390/MA16227076, 16 (2023) 7076.

[9] A. Kulshreshtha, S.K. Dhakad, Preparation of metal foam by different methods: a review, Mater. Today Proc 26 (2020) 1784–1790, https://doi.org/10.1016/J.MATPR.2020.02.375.

[10] N. Bekoz, E. Oktay, Mechanical properties of low alloy steel foams: dependency on porosity and pore size, Mater. Sci. Eng., A 576 (2013) 82–90, https://doi.org/10.1016/J.MSEA.2013.04.009.

[11] N. Tuncer, M. Bram, A. Laptev, T. Beck, A. Moser, H.P. Buchkremer, Study of metal injection molding of highly porous titanium by physical modeling and direct experiments, J. Mater. Process. Technol. 214 (2014) 1352–1360, https://doi.org/10.1016/J.JMATPROTEC.2014.02.016.

[12] M. Sahraei, A.M. Naserian-Nik, H. Sazegaran, A. Mohammad Naserian-Nik, Investigating the mechanical properties of stainless steel foams produced by dissolving spherical urea particles as a space holder, (n.d.). https://doi.org/10.21203/rs.3.rs-3394238/v2.

[13] M. sahraei, A.M. Naserian-Nik, H. Sazegaran, Investigation of the mechanical properties of stainless steel foams manufactured through leachable spherical urea granules as a space holder, Journal of Metallurgical & Materials Engineering 35 (2024) 15, https://doi.org/10.22067/JMME.2024.83785.1120.

[14] N.B. Üllen, Characterization of Cr-Mo alloyed steel foams produced by evaporative and leachable space holder techniques, Kocaeli Journal of Science and Engineering 5 (2022) 126–134, https://doi.org/10.34088/KOJOSE.1005974.

[15] A. Mansourighasri, N. Muhamad, A.B. Sulong, Processing titanium foams using tapioca starch as a space holder, J. Mater. Process. Technol. 212 (2012) 83–89, https://doi.org/10.1016/J.JMATPROTEC.2011.08.008.

[16] D. Sahu, A. Bahman, K.S. Bala Murugan, B.K. Dhurandher, A. Rai, G. Dwivedi, S. Kesharvani, Risk analysis of urea manufacturing plant using fuzzy logic approach, Proc. Inst. Mech. Eng. Part E J. Process Mech. Eng. (2024), https://doi.org/10.1177/09544089241281430/SUPPL_FILE/SJ-DOCX-1-PIE-10.1177_09544089241281430.DOCX.

[17] W.-T. Chin, W. Kroontje, Conductivity method for determination of urea, Anal. Chem. 33 (1961) 1757–1760.

[18] Y. Qin, J.M.S. Cabral, Review properties and applications of urease, biocatal, Biotransformations 20 (2002) 1–14, https://doi.org/10.1080/10242420210154.

[19] E. Urbańczyk, M. Sowa, W. Simka, Urea removal from aqueous Solutions—A review, J. Appl. Electrochem. 46 (2016) 1011–1029, https://doi.org/10.1007/S10800-016-0993-6/FIGURES/5.

[20] J.N. Sahu, K. Mahalik, A.V. Patwardhan, B.C. Meikap, Equilibrium and kinetic studies on the hydrolysis of urea for ammonia generation in a semibatch reactor, Ind. Eng. Chem. Res. 47 (2008) 4689–4696, https://doi.org/10.1021/IE800481Z.

[21] V.V. Shcherbakov, Y.M. Artemkina, E.N. Korotkova, High-frequency electric conductivity of mixtures of water with acetone, dimethyl sulfoxide, and carbamide, Russ. J. Electrochem. 50 (2014) 289–292, https://doi.org/10.1134/S1023193514030124/METRICS.

[22] C.G. Jange, C.R. Wassgren, R.P.K. Ambrose, Disintegration and release kinetics of dry compacted urea composites: a formulation and process design study, EFB Bioeconomy Journal 1 (2021) 100020, https://doi.org/10.1016/J.BIOECO.2021.100020.

[23] S. Dash, P.N. Murthy, L. Nath, P. Chowdhury, Kinetic modeling on drug release from controlled drug delivery systems, Acta Pol. Pharm. 67 (2010) 217–223. https://europepmc.org/article/med/20524422. (Accessed 1 September 2025).

[24] P. Ponnusamy, M. Loganathan, S. Krishnasamy, Mass transfer modelling and nitrogen release kinetics of nano-biochar dispersed PVA/PVP matrix encapsulated slow-release fertilizer for sustainable agriculture, Chem. Eng. J. Adv. 23 (2025) 100817, https://doi.org/10.1016/J.CEJA.2025.100817.

[25] F. Eghbali Babadi, R. Yunus, S. Masoudi Soltani, A. Shotipruk, Release mechanisms and kinetic models of gypsum-sulfur-zeolite-coated urea sealed with microcrystalline wax for regulated dissolution, ACS Omega 6 (2021) 11144–11154, https://doi.org/10.1021/ACSOMEGA.0C04353/ASSET/IMAGES/MEDIUM/AO0C04353_M016.GIF.

[26] N. Lakshani, H.S. Wijerathne, C. Sandaruwan, N. Kottegoda, V. Karunarathne, Release kinetic models and release mechanisms of controlled-release and slow-release fertilizers, ACS Agricultural Science and Technology 3 (2023) 939–956, https://doi.org/10.1021/ACSAGSCITECH.3C00152/ASSET/IMAGES/LARGE/AS3C00152_0009.JPEG.

[27] A.C. Özarslan, C. Özel, S. Yücel, Y. Basaran Elalmis, Characterizations and solubility profile of novel senary SiO2–CaO–Na2O–P2O5–CaF2–SrO glass structure modified with Nb2O5, Ceram. Int. 50 (2024) 30980–30996, https://doi.org/10.1016/J.CERAMINT.2024.05.403.

[28] S. Singh, N. Bhatnagar, A survey of fabrication and application of metallic foams (1925–2017), J. Porous Mater. 25 (2018) 537–554, https://doi.org/10.1007/S10934-017-0467-1/METRICS.

[29] H. Jain, D.P. Mondal, G. Gupta, R. Kumar, S. Singh, Synthesis and characterization of 316L stainless steel foam made through two different removal process of space holder method, Manuf. Lett. 26 (2020) 33–36, https://doi.org/10.1016/J.MFGLET.2020.09.005.

[30] M. Mirzaei, M. Hossein Paydar, Fabrication and characterization of core-shell density-graded 316L stainless steel porous structure, (n.d.). https://doi.org/10.1007/s11665-018-3797-5.

[31] H. Sazegaran, A. Feizi, M. Hojati, Effect of Cr contents on the porosity percentage, microstructure, and mechanical properties of steel foams manufactured by powder metallurgy, Trans. Indian Inst. Met. 72 (10) (2019) 2819–2826, https://doi.org/10.1007/S12666-019-01758-1, 72 (2019).

[32] G. Jia, Y. Hou, C. Chen, J. Niu, H. Zhang, H. Huang, M. Xiong, G. Yuan, Precise fabrication of open porous Mg scaffolds using NaCl templates: relationship between space holder particles, pore characteristics and mechanical behavior, Mater. Des. 140 (2018) 106–113, https://doi.org/10.1016/J.MATDES.2017.11.064.

[33] H. Jain, D.P. Mondal, G. Gupta, R. Kumar, Effect of compressive strain rate on the deformation behaviour of austenitic stainless steel foam produced by space holder technique, Mater. Chem. Phys. 259 (2021) 124010, https://doi.org/10.1016/J.MATCHEMPHYS.2020.124010.

[34] Z. Abdullah, S. Ahmad, M. Ramli, The impact of composition and sintering temperature for stainless steel foams (SS316L) fabricated by space holder method with urea as space holder, Mater. Sci. Forum 888 (2017) 413–417, https://doi.org/10.4028/WWW.SCIENTIFIC.NET/MSF.888.413.

[35] S. Joshi, G. Gupta, M. Sharma, A. Telang, T. Mahra, Synthesis and characterization of stainless steel foam via powder metallurgy taking acicular urea as space holder, Material Science Research India 12 (2015) 43–49, https://doi.org/10.13005/MSRI/120108.

[36] H. Sazegaran, M. Hojati, Effects of copper content on microstructure and mechanical properties of open-cell steel foams, Int. J. Miner. Metall. Mater. 26 (5) (2019) 588–596, https://doi.org/10.1007/S12613-019-1767-Z, 26 (2019).

[37] C.M. Hsu, Y.C. Tzeng, S.F. Chen, Y.L. Chen, H.L. Lee, Fabrication of 17-4PH stainless steel foam by a pressureless powder space holder technique, Adv. Eng. Mater. 23 (2021) 2001202, https://doi.org/10.1002/ADEM.202001202.

[38] N. Bekoz, E. Oktay, The role of pore wall microstructure and micropores on the mechanical properties of Cu–Ni–Mo based steel foams, Mater. Sci. Eng., A 612 (2014) 387–397, https://doi.org/10.1016/J.MSEA.2014.06.064.

[39] M. Stefanoni, U.M. Angst, B. Elsener, Kinetics of electrochemical dissolution of metals in porous media, Nat. Mater. 18 (2019) 942–947, https://doi.org/10.1038/S41563-019-0439-8;SUBJMETA.

[40] M.H. Sipponen, O.J. Rojas, V. Pihlajaniemi, K. Lintinen, M. Österberg, Calcium chelation of lignin from pulping spent liquor for water-resistant slow-release urea fertilizer systems, ACS Sustain. Chem. Eng. 5 (2016) 1054–1061, https://doi.org/10.1021/ACSSUSCHEMENG.6B02348.

[41] R.W. Korsmeyer, R. Gurny, E. Doelker, P. Buri, N.A. Peppas, Mechanisms of solute release from porous hydrophilic polymers, Int. J. Pharm. 15 (1983) 25–35, https://doi.org/10.1016/0378-5173(83)90064-9.

[42] J.P. Vareda, On validity, physical meaning, mechanism insights and regression of adsorption kinetic models, J. Mol. Liq. 376 (2023) 121416, https://doi.org/10.1016/J.MOLLIQ.2023.121416.

[43] T. Min, Y. Gao, L. Chen, Q. Kang, W.w.Q. Tao, Changes in porosity, permeability and surface area during rock dissolution: effects of mineralogical heterogeneity, Int. J. Heat Mass Tran. 103 (2016) 900–913, https://doi.org/10.1016/J.IJHEATMASSTRANSFER.2016.07.043.

[44] K.A. House, J.E. House, Thermodynamics of dissolution of urea in water, alcohols, and their mixtures, J. Mol. Liq. 242 (2017) 428–432, https://doi.org/10.1016/J.MOLLIQ.2017.07.020.

[45] M. Mirzaei, M.H. Paydar, A novel process for manufacturing porous 316 L stainless steel with uniform pore distribution, Mater. Des. 121 (2017) 442–449, https://doi.org/10.1016/J.MATDES.2017.02.069.

[46] N. Michailidis, F. Stergioudi, A. Tsouknidas, E. Pavlidou, Compressive response of Al-foams produced via a powder sintering process based on a leachable space-holder material, Mater. Sci. Eng., A 528 (2011) 1662–1667, https://doi.org/10.1016/J.MSEA.2010.10.088.